Heliyon 5 (2019) e03060

Contents lists available at ScienceDirect

Heliyon

journal homepage: www.cell.com/heliyon

Research article

An approximate analytical solution of the Allen-Cahn equation using homotopy perturbation method and homotopy analysis method

Safdar Hussain [a,*], Abdullah Shah [b], Sana Ayub [b], Asad Ullah [a]

[a] Department of Mathematics, Karakoram International University Gilgit, 15100, Gilgit, Pakistan
[b] Department of Mathematics, COMSATS University, Park Road, Islamabad, Pakistan

ARTICLE INFO

Keywords:
Mathematics
Chebyshev spectral method
Homotopy perturbation method
Numerical comparison
Allen-Cahn equation
Homotopy analysis method

ABSTRACT

In this paper, an approximate analytical solution of the bistable Allen–Cahn equation is given. The Allen–Cahn equation is a mathematical model to study the phase separation process in binary alloys and emerged as a convection-diffusion equation in fluid dynamics or reaction-diffusion equation in material sciences. A phase transition occurs at the interface when one material changes its composition or structure. The homotopy perturbation method and homotopy analysis method are used for finding the approximate solution. These methods don't need the use of any transformation, discretization, unrealistic restriction and assumption. The error estimates are computed by comparing with a numerical method, and a good agreement is observed.

1. Introduction

The Allen-Cahn equation is a 2nd-order nonlinear parabolic partial differential equation representing some natural physical phenomenon [1]. This equation has been extensively used to study various physical problems, such as crystal growth [2], image segmentation [3] and the motion by mean curvature flows [4]. In particular, it has become a basic model equation for the diffuse interface approach developed to study phase transitions and interfacial dynamics in material science [5]. Thus, an efficient and accurate method for the solution of this equation has practical significance and has drawn the attention of many researchers. Finding exact or numerical solutions of nonlinear and stiff differential equations is not easy. However, with the advent of modern computers and sophisticated software, we are now able to solve such kind of problems using approximate analytical or numerical techniques. Numerical techniques are somewhat complicated due to different discretization schemes and computer coding. Therefore, approximate analytical methods are becoming popular for solving nonlinear differential equations. So far, many approximate analytical methods like Variational Iteration method [6, 7, 8, 9, 10], Homotopy analysis method [11, 12, 13], Adomian decomposition method [14, 15], Homotopy perturbation method [16, 17] among others are developed for solving a large class of differential equations [18, 19, 20, 21, 22, 23, 24, 25, 26, 27, 28]. In recent years many researchers used some modified and newly developed numerical and approximate analytical techniques to study the different problems of practical interest [29, 30, 31]. They also used different methods to study the fluids flow problems mainly non-Newtonian fluids and the effect of different physical parameters on the flow [32, 33, 34, 35].

In this paper, we consider the following time-dependent equation,

$$\frac{\partial \phi}{\partial t} = \varepsilon \Delta \phi - f(\phi), \qquad (x,t) \in \Gamma \times [0,\ T], \tag{1}$$

with initial and boundary conditions,

$$\phi(x,\ 0) = f(x), \qquad \phi(a_1,\ \ t) = \phi(a_n, t) = h(t) \tag{2}$$

In the above equations, Γ is a bounded domain, the parameter ε is a small positive constant which represents the interfacial thickness. The term $f(\phi) = F'(\phi)$ with $F(\phi) = \frac{1}{4}(\phi^2 - 1)^2$ is a given double well potential. Eq. (1) describes the phase separation in binary alloys and the motion of antiphase boundaries in crystalline solids. It has become a basic model for the diffuse interface approach developed to study phase transitions and interfacial dynamics in material science.

2. Basic idea of homotopy perturbation method

In order to elaborate this method, we suppose the function given as;

$$P(\varphi) - g(x,t) = 0, \qquad t \in [0,\ T] \tag{3}$$

subject to the boundary conditions:

* Corresponding author.
E-mail address: safdar.maths@kiu.edu.pk (S. Hussain).

https://doi.org/10.1016/j.heliyon.2019.e03060
Received 16 January 2019; Received in revised form 17 August 2019; Accepted 12 December 2019

$$\beta\left(\varphi,\ \frac{\partial\varphi}{\partial n}\right)=0. \tag{4}$$

where p is a differential operator, $g(x,t)$ is known analytic function and β is boundary operator. The operator p can be further separated into linear and nonlinear operators, $L(\varphi)$ and $N(\varphi)$respectively. Therefore, Eq. (3) can be written as:

$$L(\varphi)+N(\phi)-g(x,\ t)=0 \tag{5}$$

We define a homotopy $\varphi(x,t;q):\Gamma\times[0,1]\to\mathbb{R}$ which satisfies:

$$H(\varphi(x,t;q))=(1-q)[L(\varphi)-L(\varphi_0)]+q[N(\varphi)-g(x,t)],\quad t\in[0,\ T] \tag{6}$$

where $q\in[0,1]$ and is known as an embedding parameter, and φ_0 is an initial approximation of Eq. (3). From Eq. (6), with $q=0$ and $q=1$, we will have respectively:

$$H(\varphi(x,t;0))=[L(\varphi)-L(\varphi_0)]=0 \tag{7}$$

$$H(\varphi(x,t;1))=[N(\varphi)-g(\varphi)]=0 \tag{8}$$

The variation of q from zero to one is same as change of $\varphi(x,t)$ from $\varphi_0(x,t)$ to $\varphi(x,t)$. In topology, this is called deformation, while the terms $L(\varphi)-L(\varphi_0)$ and $N(\varphi)-g(\varphi)$ are called homotopy. By using HPM, we assume that the solution of Eq. (6) can be written as a power series in q:

$$\varphi(x,t)=\varphi_0(x,t)+q\varphi_1(x,t)+q^2\varphi_2(x,t)+\ldots \tag{9}$$

Now setting $q\to1$, Eq. (9) yields:

$$\varphi(x,t)=\lim_{q\to1}\left[\varphi_0(x,t)+q\varphi_1(x,t)+q^2\varphi_2(x,t)+\ldots\right]=\varphi_0(x,t)+\varphi_1(x,t)+\varphi_2(x,t)+\ldots \tag{10}$$

In most cases, the series in Eq. (10) is convergent. For further details about convergence of the series solution obtained by using HPM the interested readers may referred to [36] and the reference there in. The unknowns$\varphi_0(x,t),\ \varphi_1(x,t),\ \varphi_2(x,t),\ldots$ can be calculated by comparing the like powers of q in Eq. (6).

3. Basic idea of homotopy analysis method

Let us consider the following nonlinear equation

$$N[\psi(x,t)]=0. \tag{11}$$

Where $N$is nonlinear operator, x and t are independent variables and $\psi(x,t)$ is the unknown function. By means of generalizing the traditional homotopy method, Liao [11] constructed the zero-order deformation equation as follows:

$$(1-p)L[\psi(x,t;p)-\psi_0(x,t)]=phH(x,t)N[\psi(x,t;p)]=0. \tag{12}$$

Where $p\in[0,1]$is the embedding parameter, $h\neq0$ is a non-zero auxiliary parameter, $H(x,t)\neq0$ is an auxiliary function, L is linear operator and $\psi_0(x,t)$ is the initial guess of $\psi(x,t)$. When $p=0$and $p=1$, Eq. (12) gives

$$\psi(x,t;0)=\psi_0(x,t),\qquad \psi(x,t;1)=\psi(x,t). \tag{13}$$

Now expanding $\psi(x,t;p)$ with respect to$p$ by Taylor series, we have

$$\psi(x,t;p)=\psi_0(x,t)+\sum_{n=1}^{+\infty}\psi_n(x,t)p^n, \tag{14}$$

where

$$\psi_n(x,t)=\frac{1}{n!}\frac{\partial^n\psi(x,t;p)}{\partial p^n}\bigg|_{p=0}. \tag{15}$$

If we choose the linear operator$L$, the initial guess$\psi_0(x,t)$, the auxiliary parameter h and the auxiliary function $H(x,t)$ properly, the series (14) converges at$p=1$, then we get

$$\psi(x,t)=\psi_0(x,t)+\sum_{n=1}^{+\infty}\psi_n(x,t). \tag{16}$$

Define the vector

$$\overrightarrow{\psi}(x,t)=\{\psi_0(x,t),\ \psi_1(x,t),\ \psi_2(x,t),\ldots,\ \psi_n(x,t)\}. \tag{17}$$

The n$^{\text{th}}$-order deformation equation obtained using Eq. (12) is given as,

$$L[\psi_n-\lambda_n\psi_{n-1}]=hH(x,t)R_n[\overrightarrow{\psi}_{n-1}]. \tag{18}$$

Where

$$R_n[\overrightarrow{\psi}_{n-1}]=\frac{1}{(n-1)!}\frac{\partial^{n-1}N[\psi(x,t;p)]}{\partial p^{n-1}} \tag{19}$$

and

$$\lambda_n=\begin{cases}0, & n=1\\ 1, & n>1\end{cases}. \tag{20}$$

Now applying L^{-1}on both sides of Eq. (18) and simplifying, we get

$$\psi_n(x,t)=hL^{-1}\{H(x,t)R_n[\overrightarrow{\psi}_{n-1}]\}+\lambda_n\psi_{n-1}. \tag{21}$$

In this way one can easily obtain the approximate solution $u(x,t)$ of the form

$$\psi(x,t)=\sum_{n=0}^{N}\psi_n(x,t), \tag{22}$$

where $\psi_n(x,t)$ can be obtained by solving Eq. (21).

4. Solution of the Allen-Cahn equation using homotopy perturbation method

In this section, we solve the Allen-Cahn equation with different initial and boundary conditions using HPM.

4.1. Example 1

Consider the Allen-Cahn equation of the form [37],

$$u_t(x,t)=\varepsilon u_{xx}(x,\ t)+u(x,t)-u^3(x,t),\qquad x\in[-1,\ 1],\qquad t>0 \tag{23}$$

with the initial condition,

$$u(x,0)=0.53x+0.47\sin(-1.5\pi x) \tag{24}$$

By choosing initial condition as an initial guess, i.e.,

$$u_0^*(x,t)=0.53x+0.47\sin(-1.5\pi x) \tag{25}$$

which satisfy the boundary conditions,

$$u(-1,t)=-1,\qquad u(1,t)=1 \tag{26}$$

The homotopy expression for Eq. (23) will be,

$$(1-p)\left[\dot{u}-\dot{u}^*_0\right]+p\left[\dot{u}-\varepsilon^2u''-u+u^3\right]=0, \tag{27}$$

here $\dot{u}=\frac{\partial u}{\partial t}$, and $u''=\frac{\partial^2u}{\partial x^2}$.

Now consider the series solution of Eq. (23) is of the form,

$$u(x,t)=u_0+pu_1+p^2u_2+p^3u_3+p^4u_4+\ldots \tag{28}$$

Taking limit $p\to1$ in Eq. (28), we get,

$$u(x,t) = u_0 + u_1 + u_2 + u_3 + u_4 + \ldots \tag{29}$$

Using Eq. (28) in Eq. (27) and comparing the like powers of embedding parameter 'p', we get the following system of equations,

$$O(p^0), \qquad \frac{\partial u_0}{\partial t} - \frac{\partial u_0^*}{\partial t} = 0, \tag{30}$$

$$O(p^1), \qquad \frac{\partial u_1}{\partial t} + \frac{\partial u_0}{\partial t} - \varepsilon \frac{\partial^2 u_0}{\partial x^2} - u_0 + u_0^3 = 0, \tag{31}$$

$$O(p^2), \qquad \frac{\partial u_2}{\partial t} - \varepsilon \frac{\partial^2 u_1}{\partial x^2} - u_1 + 3u_0^2 u_1 = 0. \tag{32}$$

Solving Eqs. (30), (31), and (32), we get the following solutions,

$$u_0 = u_0^* = 0.54x + 0.47\sin(-1.5\pi x), \tag{33}$$

4.2. Graphical representation

Figure 1 and Figure 2 show the comparison of approximate analytical solution using HPM and numerical solution obtained by solving the Allen Cahn equation using Chebyshev spectral method [19] for different time scales at $\varepsilon = 0.001$. The Figure 3 show the surface plot.

4.3. Example 2

Next, we consider the Allen-Cahn equation with different initial and boundary conditions [29];

$$u_t(x,t) = \varepsilon u_{xx}(x,\ t) + u(x,t) - u^3(x,t), \qquad x \in [0,\ 2\pi], \qquad t > 0, \tag{37}$$

with the initial condition

$$u(x,\ 0) = 0.25\sin(x) \tag{38}$$

Here, we will use initial condition as an initial guess,

$$u_1 = (10.43710666\varepsilon^2\sin(4.712388981x) + 0.53x - 0.47\sin(4.712388981x) - (0.53x - 0.47\sin(4.712388981x))^3)t, \tag{34}$$

$$\begin{aligned} u_2 = 5\varepsilon^2\big(& -231.7727562\varepsilon^2\sin\big(4.712388981x\big) + 10.43710666\sin\big(4.712388981x\big) \\ & -6(0.53x - 0.47\sin(4.712388981x))(0.53 - 2.214822821\cos(4.712388981x))^2 \\ & -31.31131998(0.53x - 0.47\sin(4.712388981x))^2\sin\big(4.712388981x\big)\big)t^2 \\ & +0.5\big(10.43710666\varepsilon^2\sin\big(4.712388981x\big) + 0.53x - 0.47\sin\big(4.712388981x\big) \\ & -(0.53x - 0.47\sin(4.712388981x))^3\big)t^2 - 1.5\big(10.43710666\varepsilon^2\sin\big(4.712388981x\big) + .53x \\ & -0.47\sin(4.712388981x) - (0.53x - 0.47\sin(4.712388981x))^3\big)t^2\big(0.53x - 0.47\sin\big(4.712388981x\big)\big)^2. \end{aligned} \tag{35}$$

Similarly we can calculate $u_3,\ u_4,\ u_5\ldots$ to get the required accuracy.

Substituting the values of $u_0,\ u_1,\ u_2$ from Eqs. (33), (34), and (35) in Eq. (29) to get the approximate analytical solution of the form;

$$\begin{aligned} u(x,t) = {} & 0.54x + 0.47\sin(-1.5\pi x) + \big(10.43710666\varepsilon^2\sin\big(4.712388981x\big) + 0.53x \\ & -0.47\sin(4.712388981x) - (0.53x - 0.47\sin(4.712388981x))^3\big)t \\ & +5\varepsilon\big(-231.7727562\varepsilon\sin(4.712388981x) + 10.43710666\sin(4.712388981x) \\ & -6(0.53x - 0.47\sin(4.712388981x))(0.53 - 2.214822821\cos(4.712388981x))^2 \\ & -31.31131998(0.53x - 0.47\sin(4.712388981x))^2\sin\big(4.712388981x\big)\big)t^2 \\ & +0.5(10.43710666\varepsilon\sin(4.712388981x) + 0.53x - 0.47\sin(4.712388981x) \\ & -(0.53x - 0.47\sin(4.712388981x))^3)t^2 - 1.5(10.43710666\varepsilon\sin(4.712388981x) \\ & +.53x - 0.47\sin(4.712388981x) - (0.53x - 0.47\sin(4.712388981x))^3\big)t^2 \\ & (0.53x - 0.47\sin(4.712388981x))^2. \end{aligned} \tag{36}$$

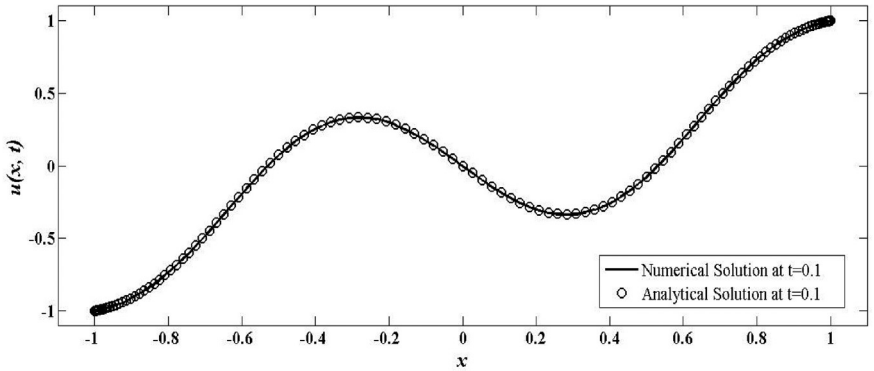

Figure 1. Comparison of numerical solution and HPM solution at $t = 0.1$ and.$\varepsilon = 0.001$.

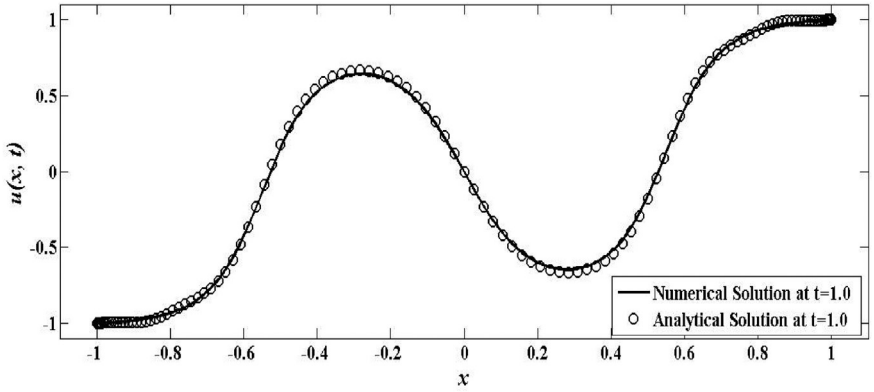

Figure 2. Comparison of numerical solution and HPM solution at $t = 1.0$ and.$\varepsilon = 0.001$.

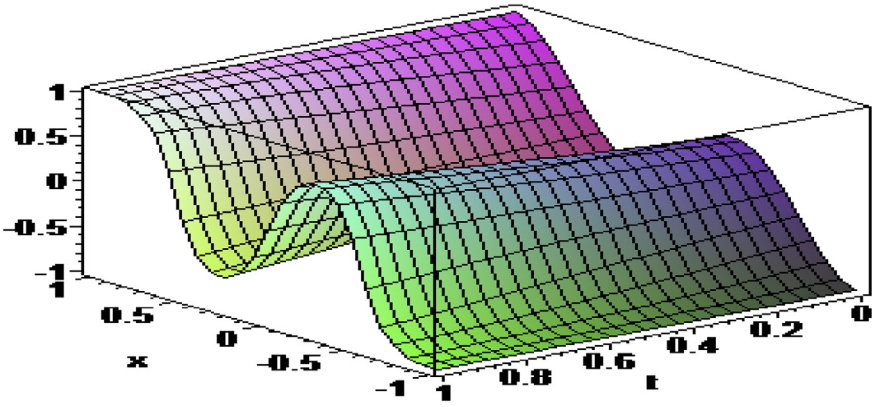

Figure 3. Homotopy perturbation solution for $u(x,t)$for the first five approximations when.$\varepsilon = 0.001, \quad x \in [-1,1] \quad and \quad 0 \le t \le 1$.

$$u_0^* = 0.25\,\sin(x), \tag{39}$$

with the homogeneous boundary conditions,

$$u(0,\quad t) = 0, \qquad u(2\pi,\quad t) = 0. \tag{40}$$

The homotopy expression for Eq. (37) will be,

$$(1-p)\left[\dot{u} - \dot{u}_0^*\right] + p\left[\dot{u} - \varepsilon u'' - u + u^3\right] = 0. \tag{41}$$

Now consider the series solution of Eq. (37) as in Eq. (28). Using Eq. (28) in Eq. (41) and comparing the like powers of embedding parameter 'p', we get the following system of equations;

$$O(p^0), \qquad \frac{\partial u_0}{\partial t} - \frac{\partial u_0^*}{\partial t} = 0, \tag{42}$$

$$O(p^1), \qquad \frac{\partial u_1}{\partial t} - \varepsilon\frac{\partial^2 u_0}{\partial x^2} - u_0 + u_0^3 = 0, \tag{43}$$

$$O(p^1), \qquad \frac{\partial u_2}{\partial t} - \varepsilon\frac{\partial^2 u_1}{\partial x^2} - u_1 + 3u_0^2 u_1 = 0. \tag{44}$$

Solving Eqs. (42), (43), and (44), we get the following solutions;

$$u_0 = u_0^* = 0.25\,\sin(x), \tag{45}$$

$$u_1 = t(-0.25\varepsilon\sin(x) + 0.25\sin(x) - 0.015625\sin(x)^3), \tag{46}$$

$$\begin{aligned} u_2 = {} & 0.5\varepsilon(0.25\varepsilon\sin(x) - 0.25\sin(x) - 0.09375\sin(x)\cos(x)^2 + 0.046875\sin(x)^3)t^2 \\ & +0.5(-0.25\varepsilon\sin(x) + 0.25\sin(x) - 0.015625\sin(x)^3)t^2 - 0.09375\sin(x)^2(-0.25\varepsilon\sin(x) \\ & +0.25\sin(x) - 0.015625\sin(x)^3)t^2. \end{aligned} \tag{47}$$

Similarly, we can calculate $u_3,\ u_4,\ u_5\ldots$ to get the required accuracy.

Substituting the values of $u_0,\quad u_1,\quad u_2$ from Eqs. (45), (46), and (47) in Eq. (29) we get the approximate analytical solution as;

$$\begin{aligned} u(x,t) = {} & 0.25\,\sin(x) + t(-0.25\varepsilon\sin(x) + 0.25\sin(x) - 0.015625\sin(x)^3) \\ & +0.5\varepsilon(0.25\varepsilon\sin(x) - 0.25\sin(x) - 0.09375\sin(x)\cos(x)^2 + 0.046875\sin(x)^3)t^2 \\ & +0.5(-0.25\varepsilon\sin(x) + 0.25\sin(x) - 0.015625\sin(x)^3)t^2 - 0.09375\sin(x)^2(-0.25\varepsilon\sin(x) \\ & +0.25\sin(x) - 0.015625\sin(x)^3)t^2. \end{aligned} \tag{48}$$

4.4. Graphical representation

Figure 4 and Figure 5 show the comparison of approximate analytical solution using HPM and numerical solution obtained by Chebyshev collocation method [19] for different time scales at $\varepsilon = 0.001$. Figure 6 show surface plot.

5. Solution of the Allen Cahn equation using homotopy analysis method

In this section we will solve above examples using HAM and will compare the results with the HPM through absolute error tables.

$$R_n(\vec{u}_{n-1}) = \left[\frac{\partial u_{n-1}}{\partial t} - \varepsilon\frac{\partial^2 u_{n-1}}{\partial x^2} - u_{n-1} + \sum_{j=0}^{n-1} u_{n-1-j}\left(\sum_{k=0}^{j} u_{j-1-k}u_k\right)\right]. \tag{50}$$

For $n = 1$, Eq. (49) and Eq. (50) gives;

$$u_1(x,t) = hL^{-1}\{H(x,t)R_1[\vec{u}_0]\} + \lambda_0 u_0, \tag{51}$$

$$R_1[\vec{u}_0] = \frac{\partial u_0}{\partial t} - \nu\frac{\partial^3 u_0}{\partial x^2 \partial t} + \frac{\partial^4 u_0}{\partial x^4} - \frac{\partial^2}{\partial x^2}\left({u_0}^3 - u_0\right). \tag{52}$$

In order to obey both the rule of solution expression and the rule of the coefficient ergodicity [11], the corresponding auxiliary function can be determined uniquely $H(x, t)=1$. Using Eq. (25) in Eq. (52) to get $R_1[\vec{u}_0]$ and then using the value of $R_1[\vec{u}_0]$ in Eq. (51), we obtain first approximation,

$$\begin{aligned} u_1 = h(&-10.43710666\varepsilon\ \sin(4.712388981\mathrm{x}) - 0.53\mathrm{x} + 0.47\sin(4.712388981\mathrm{x}) \\ &+(0.53\mathrm{x} - 0.47\sin(4.712388981\mathrm{x}))^3)\mathrm{t}. \end{aligned} \tag{53}$$

Similarly, for $n = 2$, we get second approximation

$$\begin{aligned} u_2(x,t) = h(&h(10.43710666\varepsilon\ \sin(4.712388981x) - 0.53x + .47\ \sin(4.712388981x) \\ &+(0.53x - 0.47\ \sin(4.712388981x))^3)t\ - 0.5\varepsilon\, h(231.7727562\varepsilon\ \sin(4.712388981x) \\ &+10.43710666\ \sin(4.712388981x) + 6(0.53x - 0.47\ \sin(4.712388981x)) \\ &+(0.53 - 2.214822821\ \cos(4.712388981x))^2 + 31.31131998\left(0.53x - 0.47\ \sin\left(4.712388981x\right)\right)^2 \sin\left(4.712388981x\right)\Big)t^2. \end{aligned} \tag{54}$$

5.1. Example 1

Here we repeat example (1) as represented in Eq. (23) along with given initial and boundary conditions. Using Eqs. (19) and (21), we can write nth order deformation equation for Eq. (23) given below;

$$u_n(x,t) = hL^{-1}\{H(x,t)R_n(\vec{u}_{n-1})\} + \lambda_n u_{n-1}, \tag{49}$$

where

Continuing in a similar manner we can find for $n = 3, 4, 5\ldots$ and the final solution will be:

$$u(x,\ t) = u_0(x,t) + \ u_1(x,t) + \ \ u_2(x,t) + \ldots \tag{55}$$

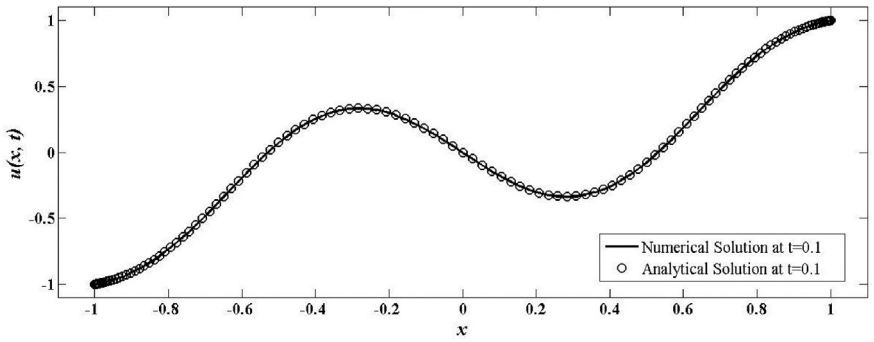

Figure 4. Comparison of numerical solution and HPM solution at $t = 0.1$.

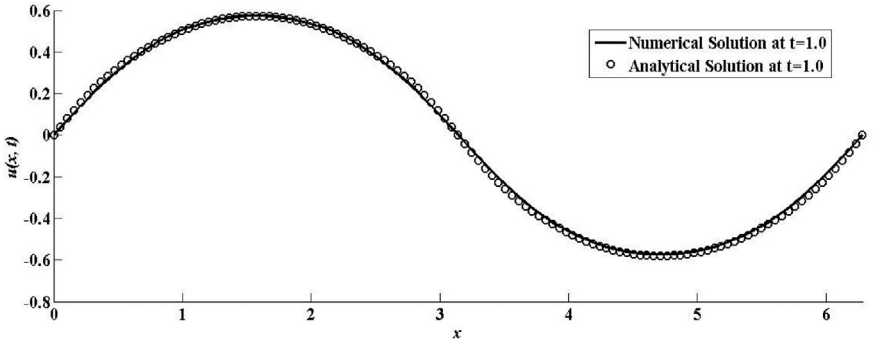

Figure 5. Comparison of numerical solution and HPM solution at $t = 1.0$ and.$\varepsilon = 0.001$.

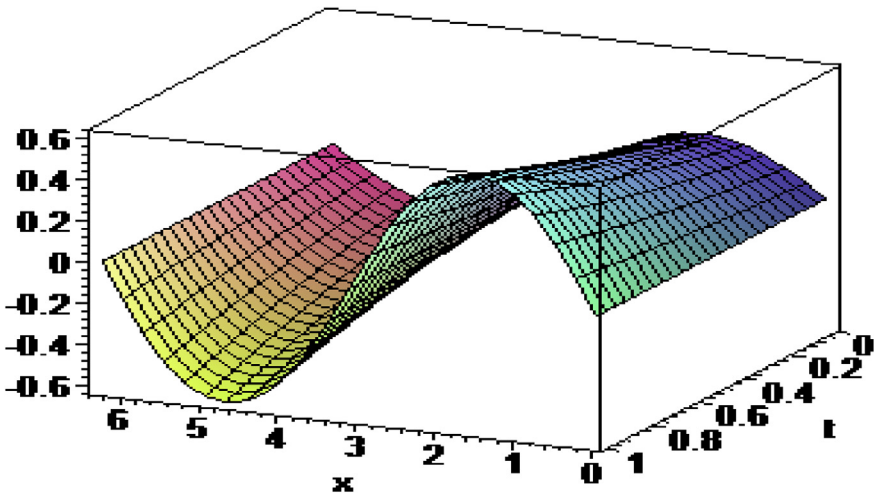

Figure 6. Describes the homotopy Analysis results for $u(x,t)$for the first five approximations when.$\varepsilon = 0.001,\ \ x \in [0,\ 2\pi]\ \ and\ \ 0 \leq t \leq 1$.

5.2. h-curves of the HAM solution for example (1)

The convergence and rate of approximation for the HAM solution strongly depends on the values of auxiliary parameter 'h'. It is straightforward to choose a proper value of h which ensure that the solution series is convergent. It is easy to discover the valid region of h, which corresponds to the line segments nearly parallel to the horizontal axis [11]. Here h-curve is plotted after 5th-order of HAM approximations when$\varepsilon = 0.001$, t = 0.5 and x = -1. Figure 7 clearly depicts the range for admissible values of 'h' is -2.5 < h < 1.5.

5.3. Absolute error analysis

In this section, we demonstrate how close an approximate solutions of the Alen-Cahn equation obtained using HPM and HAM. In Table 1 and Table 2 we have presented absolute error.

5.4. Effect of thickness parameter on solution

The effect of thickness parameter is studied in Figure 8, clearly this figure show the behaviour of solution for different values of thickness parameter ε at t = 0.5.

Table 1. The absolute error between the solutions obtained by using HPM and HAM after fifth order approximations, taking $h = -1$ and.$\varepsilon = 0.001$.

t_n/x_n	0.00	0.2	0.4	0.6	0.8	1.0
-1	0.00	1×10^{-10}	0.00	2×10^{-10}	7×10^{-10}	1×10^{-9}
-0.5	0.00	0.00	1×10^{-10}	1×10^{-10}	1×10^{-10}	1×10^{-10}
0.00	0.00	0.00	0.00	0.00	0.00	0.00
0.5	0.00	1×10^{-10}	1×10^{-10}	1×10^{-10}	1×10^{-9}	0.00
1	0.00	1×10^{-10}	1×10^{-10}	1×10^{-10}	1×10^{-9}	0.00

Table 2. The absolute error between the solutions obtained by using HPM and HAM after fifth order approximations, taking $h = -1$ and.$\varepsilon = 0.001$.

t_n/x_n	0.00	0.2	0.4	0.6	0.8	1.0
0	0.00	0.00	0.00	0.00	0.00	0.00
$\pi/2$	0.00	1×10^{-10}	1×10^{-10}	1×10^{-10}	0.00	1×10^{-10}
$3\pi/2$	0.00	1×10^{-10}	1×10^{-10}	1×10^{-10}	0.00	1×10^{-10}
2π	0.00	0.00	0.00	0.00	0.00	0.00

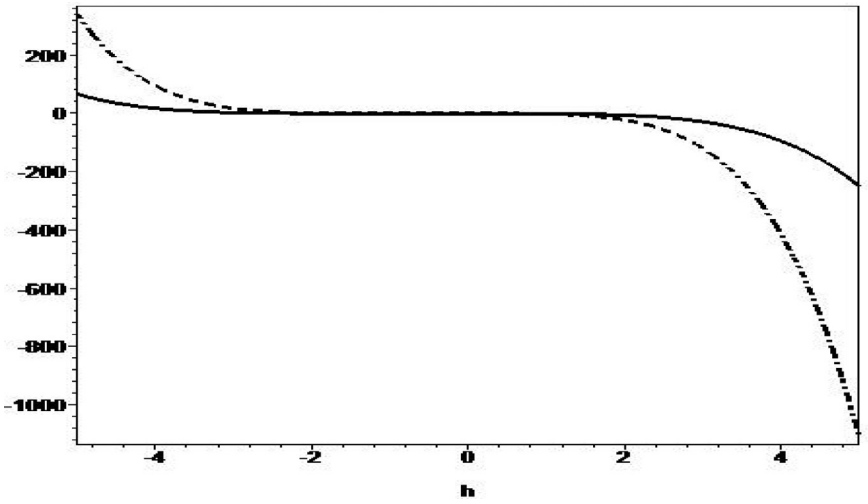

Figure 7. h-curve of $u(x,\ t)$ denoted by dashed line and $u_t(x,\ t)$ denoted by solid line.

6. Example 2

In this section we repeat example (2) as presented in Eq. (37) along with given initial and boundary conditions.

From Eqs. (19) and (21), we can write nth order deformation equation for Eq. (37) is given below;

$$u_n(x,t) = hL^{-1}\{H(x,t)R_n(\vec{u}_{n-1})\} + \lambda_n u_{n-1}, \tag{56}$$

where

$$R_n(\vec{u}_{n-1}) = \left[\frac{\partial u_{n-1}}{\partial t} - \varepsilon\frac{\partial^2 u_{n-1}}{\partial x^2} - u_{n-1} + \sum_{j=0}^{n-1} u_{n-1-j}\left(\sum_{k=0}^{j} u_{j-1-k}u_k\right)\right] \tag{57}$$

$$u_1(x,t) = hL^{-1}\{H(x,t)R_1[\vec{u}_0]\} + \lambda_0 u_0, \tag{58}$$

$$R_1[\vec{u}_0] = \frac{\partial u_0}{\partial t} - \varepsilon\frac{\partial^3 u_0}{\partial x^2} - u_0 + u_0^3. \tag{59}$$

Using Eq. (39) in Eq. (59) and then using the result obtained in Eq. (58), we obtain first approximation,

$$u_1 = h(0.25\varepsilon\sin(x) - .25\sin(x) + 0.015625\sin(x)^3). \tag{60}$$

Similarly, for$n = 2$, we get second approximation,

$$\begin{aligned} u_2(x,t) = {} & h(h(0.25\varepsilon\sin(x) - 0.25\sin(x) + 0.015625\sin(x)^3)\mathrm{t} \\ & -0.5\varepsilon h(-\varepsilon\sin(x) + 0.25\sin(x) + 0.09375\sin(x)\cos(x)^2 - 0.046875\sin(x)^3)\mathrm{t}^2 \\ & -0.5h(0.25\varepsilon\sin(x) - 0.25\sin(x) + 0.015625\sin(x)^3)\mathrm{t}^2 + 0.09375\sin(x)^2 h(0.25\varepsilon\sin(x) \\ & -0.25\varepsilon\sin(x) + 0.015625\sin(x)^3)\mathrm{t}^2) + h(0.25\varepsilon\sin(x) - 0.25\sin(x) + 0.015625\sin(x)^3)\mathrm{t}. \end{aligned} \tag{61}$$

Again from example 2, we assume$H(x,t) = 1$.
For $n = 1$, Eq. (56) and Eq. (57) gives;

Continuing in a similar manner we can find $u_3(x,t)$, $u_4(x,t)$, $u_5(x,t)$, ...for$n = 2, 3, 4, ...$and the final solution will be;

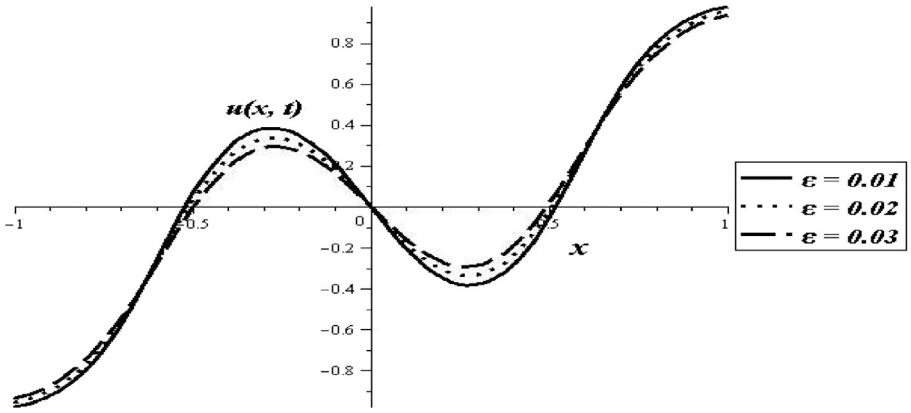

Figure 8. Impact of thickness parameter on solution *u(x, t)*.

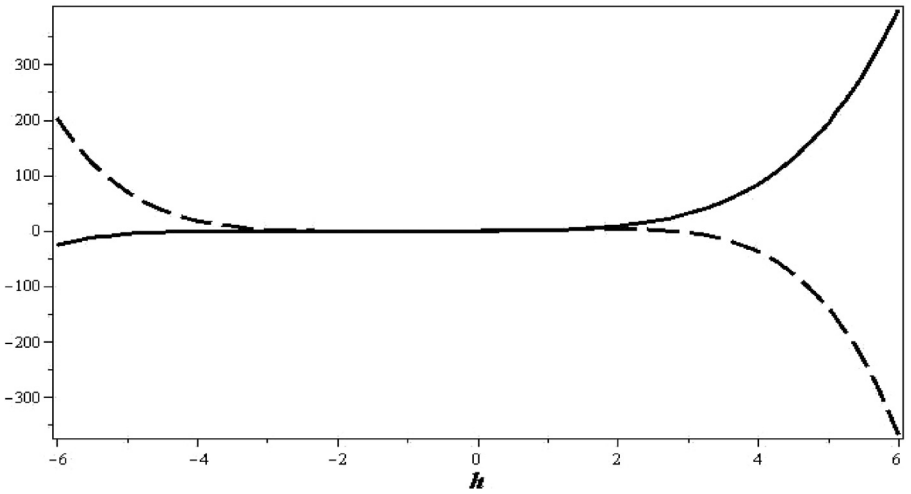

Figure 9. h-curve of $u(u,t)$ dashed line and.$u_t(x,t)$ solid line.

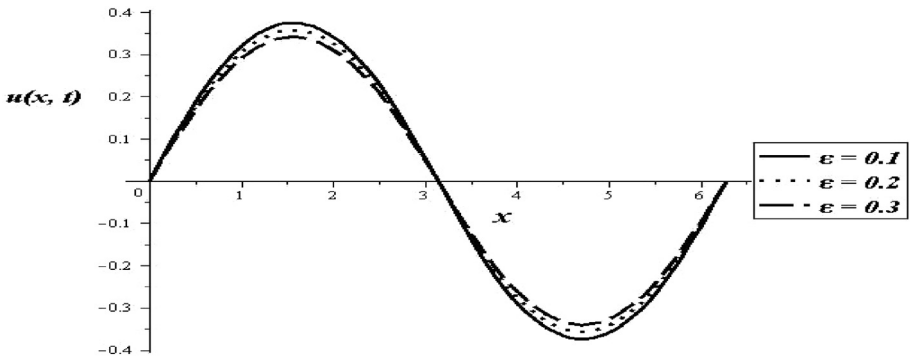

Figure 10. Figure show the behaviour of solution $u(x,\ t)$ for different values of.ε.

$$u(x,\ t) = u_0(x,t) + u_1(x,t) + u_2(x,t) + \ldots \quad (62)$$

6.1. h-curve for example 2

Here h-curve is plotted after 5th-order of HAM approximations for example (2) when$\varepsilon = 0.001$, t = 0.5 and $x = 2.5$. Figure 9 clearly show the range for admissible values of 'h' is -3 < h < 2.

6.2. Absolute error analysis

In this section absolute difference between the solution obtained by HPM and HAM for example (2) is presented.

6.3. Effect of thickness parameter on solution

The effect of thickness parameter for example (2) is studied in Figure 10, clearly this figure show the stability of solution for different values of thickness parameter ε at t = 0.5.

7. Conclusion

In this work, the HPM and HAM are successfully implemented to obtain an approximate analytical solution of the Allen-Cahn equation. Comparison has made of the obtained analytical solutions with numerical one using Chebyshev spectral method. Computed results are illustrated graphically, and a good agreement is observed. However, analytical techniques require no discretization, transformation or large computer memory when compare to numerical methods. Also, comparison between HPM and HAM is provided in tabulated form (Table 1 and Table 2) to show the accuracy of the analytical solutions. Effect of thickness parameter has also been studied for different values and illustrated graphically.

Declarations

Author Contribution Statement

S. Hussain: Conceived and designed the experiments; Wrote the paper.

A. Shah: Analyzed and interpreted the data.

S. Ayub, A. Ullah: Contributed reagents, materials, analysis tools or data. Conceived and designed the experiments; Performed the experiments; Analyzed and interpreted the data; Contributed reagents, materials, analysis tools or data; Wrote the paper.

Funding Statement

This research did not receive any specific grant from funding agencies in the public, commercial, or not-for-profit sectors.

Competing Interest Statement

The authors declare no conflict of interest.

Additional Information

No additional information is available for this paper.

References

[1] S. Allen, J.W. Cahn, A microscopic theory for antiphase boundary motion and its application to antiphase domain coarsening, Acta Metall. 27 (1979) 1085–1095.
[2] Abdullah Shah, Muhammad Sabir, Bastain Peter, An efficient time-stepping scheme for numerical simulation of dendritic crystal growth, Eur. J. Comput. Mech. 25 (6) (2017) 475–488.
[3] M. Benes, V. Chalupecky, K. Mikula, Geometrical image segmentation by the Allen–Cahn equation, Appl. Numer. Math. 51 (2) (2004) 187–205.
[4] Abdullah Shah, Muhammad Sabir, Muhammad Qasim, Peter Bastain, Efficient numerical scheme for solving the Allen-Cahn equation, Numer. Methods Partial. Differ. Equ. 34 (2018) 1820–1833.
[5] Abdullah Shah, Li Yuan, Numerical solution of a phase-field model for incompressible two-phase flows based on artificial compressibility, Comput. Fluids 42 (1) (2011) 54–61.
[6] J.H. He, Variational iteration method some recent results and new interpretations, J. Comput. Appl. Math. 207 (2007) 3–17.
[7] A.M. Wazwaz, The variational iteration method for rational solutions for KdV, K(2,2), burgers and cubic boussinesq equations, J. Comput. Appl. Math. 207 (1) (2007) 18–23.
[8] A.M. Wazwaz, The variational iteration method: a reliable analytic tool for solving linear and nonlinear wave equations, Comput. Math. Appl. 54 (7–8) (2007) 926–932.
[9] A.M. Wazwaz, The variational iteration method for solving linear and nonlinear systems of PDEs, Comput. Math. Appl. 54 (7–8) (2007) 895–902.
[10] Abdullah Shah, S. Khlil, S. Hussain, An efficient iterative technique for solving some nonlinear problems, Int. J. of Nonlinear Sci. 13 (1) (2012).
[11] S.J. Liao, Beyond Perturbation: Introduction to the Homotopy Analysis Method, CRC Press, Boca Raton, 2003. Chapman & Hall.
[12] S.J. Liao, The Proposed Homotopy Snalysis Technique for the Solution of Nonlinear Problems, Ph.D. Thesis, Shanghai Jiao Tong University, 1992.
[13] S.J. Liao, Comparison between the homotopy analysis method and homotopy perturbation method, Appl. Math. Comput. 169 (2005) 1186–1194.
[14] G.A. Adomian, Review of the decomposition method in applied mathematics, J. Math. Anal. Appl. 135 (1988) 501–544.
[15] A. Repaci, Nonlinear dynamical systems: on the accuracy of Adomian's decomposition method, Appl. Math. Lett. 3 (3) (1990) 35–39.
[16] J.H. He, A coupling method of homotopy technique and perturbation technique for nonlinear problems, Int. J. Non-Linear Mech. 35 (1) (2000) 37–43.
[17] J.H. He, Homotopy perturbation method for solving boundary value problems, Phys. Lett. A 350 (2006) 87–88.
[18] O. Ozdemir, M.O. Kaya, Flapwise bending vibration analysis of a rotating tapered cantilever Bernouli-Euler beam by differential transform method, J. Sound Vib. 289 (2006) 413–420.
[19] L.N. Trefethen, Spectral Methods in Matlab, Oxford University, Oxford, England, 2000.
[20] V.Z. Gristchak, V.Z. Ye, M. Dmitrieva, A hybrid WKB-galerkin method and its application, Tech. Mech. 15 (1995) 281–294.
[21] E. Tadmor, The exponential accuracy of Fourier and Chebyshev differencing methods, SIAM. Numer. Anal. 23 (1986) 1–10.
[22] I.H. Abdel-Halim Hassan, Application to differential transformation method for solving systems of differential equations, Appl. Math. Model. 32 (12) (2008) 2552–2559.
[23] M. Zaid, Odibat, Differential transform method for solving Volterra integral equation with separable kernels, Math. Comput. Model. 7 (8) (2008) 1144–1149.

[24] A.M. Siddiqui, Abdullah Shah, Q.K. Ghori, Homotopy analysis of slider bearing lubricated with powell-eyring fluid, J. Appl. Sci. 6 (11) (2006) 2358–2367.
[25] S. Hussain, Abdullah Shah, An analysis of two iterative techniques for solution of Cahn-Hilliard equation, Int. J. of Nonlinear Sci. 12 (1) (2011) 42–47.
[26] W. Malfliet, The tanh method: a tool for solving certain classes of nonlinear evolution and wave equations, J. Comput. Appl. Math. (164–165) (2004) 529–541.
[27] Haofeng Li, Wenzhen Chen, Qian Zhu, Lei Luo, Exponential function method for solving point reactor neutron kinetics equations, Nucl. Power Eng. 30 (4) (2009) 28–31.
[28] J. Biazar, H. Ghazvini, Convergence of the homotopy perturbation method for partial differential equations, Nonlinear Anal. Real World Appl. 10 (2009) 2633–2640.
[29] B. Marinca, V. Marinca, New exact and explicit solutions of the zakharov equations and generalized zakharov equations by the quotient trigonometric function expansion method, Proc. Rom. Acad. Ser. A 18 (2017) 166–173.
[30] N. Herisanu, V. Marinca, G. Madescu, Gheorghe, F. Dragan, Dynamic response of a permanent magnet synchronous generator to a wind gust, Energies 12 (5) (2019) 915.
[31] N. Herisanu, V. Marinca, An iteration procedure with application to Van der Pol oscillator, Int. J. Nonlinear Sci. Numer. Stimul. 10 (2009) 353–361.
[32] B. Marinca, V. Marinca, Approximate analytical solutions for thin film flow of a fourth grade fluid down a vertical cylinder, Proc. Rom. Acad. Ser. A 19 (2018) 69–76.
[33] B. Marinca, V. Marinca, Optimal auxiliary functions method for nonlinear thin film flow of a third grade fluid on a moving belt, Proc. Rom. Acad. Ser. A 19 (2018) 575–580.
[34] V. Marinca, Vasile, N. Herişanu, On the flow of a Walters-type B' viscoelastic fluid in a vertical channel with porous wall, Int. J. Heat Mass Transf. 79 (2014) 146–165.
[35] M.I. Khan, F. Haq, T. Hayat, A. Alsaedi, M. Rahman, Natural bio-convective flow of Sisko nanofluid subject to gyrotactic microorganisms and activation energy, Phys. Scr. (2019).
[36] J. Biazar, H. Ghazvini, Convergence of the homotopy perturbation method for partial differential equations, Nonlinear Anal. Real World Appl. 10 (2009) 2633–2640.
[37] S. Huailing, J. Lijian, L. Qiuqi, A reduced order method for Allen–Cahn equations, J. Comput. Appl. Math. 292 (2016) 213–229.